JOURNAL OF MATERIALS SCIENCE **34** (1999) 3479–3487

Photoelastic studies for composite dynamics

LIU HAIXIAO*‡, ZHANG CHUHAN§, LI ZHENG¶, ZHOU XTRENG*
*Department of Port Engineering, Tianjin University, Tianjin 300072, People's Republic of China
§Department of Hydraulic Engineering and Hydropower, Tsinghua University, Beijing 100084, People's Republic of China
¶Department of Mechanics, Beijing University, Beijing 100871, People's Republic of China

The orthotropic birefringent composites suitable for the study of dynamic photoelasticity are investigated and the determination of residual birefringence in the materials is briefly described. A stress-optic law for dynamic photoelastic analysis of orthotropic birefringent composites is postulated based on the static stress-optic law of Hyer and Liu. Subsequently, practical methods of calibrating dynamic mechanical constants and dynamic stress-fringe values are proposed. With dynamic strain measurements and time domain BEM for anisotropic media, three calibration specimens (0°, 90° and 45°) are used to verify the proposed stress-optic law in uniaxial-stress fields and a plate of unidirectional fiber-reinforced birefringent composite under impact loading, with the loading direction parallel, perpendicular and at 45° to the fiber direction, is analyzed to verify the proposed stress-optic law in biaxial-stress fields. Results show that the dynamic stress-optic law for orthotropic birefringent composites is valid in the two cases. © *1999 Kluwer Academic Publishers*

1. Introduction

Considerable work has been performed over the past years on the development of orthotropic birefringent material and the development of stress (strain)-optic law which characterize relations between the optical and mechanical responses of the material. However, few efforts were made in dynamic analysis of birefringent composites. There were only preliminary researches on the phenomenon of wave propagation in birefringent composites [1, 2]. Dally, Link and Prabhakaran obtained dynamic birefringent fringe patterns in fiber-reinforced birefringent composites by employing pulsed-laser illumination in the early seventies. They observed several kinds of waves which are similar to those observed in isotropic birefringent materials. Dynamic analysis of birefringent composites is very valuable in the fields of earthquake engineering, rock dynamics and dynamic composite research. However, it is faced with some new problems which are not existent in dynamic analysis for isotropic birefringent materials and in static analysis for orthotropic birefringent composites, such as orthotropic birefringent composites suitable for dynamic analysis, the effects of residual birefringence in materials, dynamic stress (strain)-optic law and calibrations of dynamic mechanical constants and dynamic stress-fringe values for orthotropic birefringent composites. The purpose of this paper is to study the above problems, especially the dynamic stress-optic law for orthotropic birefringent composites. Furthermore, with dynamic strain measurements and time domain BEM for anisotropic media, the proposed dynamic stress-optic law is verified in uniaxial-stress and biaxial-stress fields.

2. Dynamic stress-optic law

Three categories of orthotropic stress (strain)-optic laws, which include almost all kinds of interpretations of the photoelastic effect observed in orthotropic birefringent composites, can be classified in the development of static orthotropic photoelasticity. They are represented by Sampson's stress-optic law, Prabhakaran's strain-optic law and Hyer and Liu's stress-optic law, respectively.

In composites, residual birefringence is a result of residual stresses which arise from differences in the thermal-expansion coefficients of composites constituents and from volume contraction of the resin during the cure. Neither Sampson's stress-optic law nor Prabhakaran's strain-optic law takes the effects of the residual birefringence into account. Studies [3–6] have shown that it is the reason that led to the disparity between experimental and predicted results as these two laws were accepted. The first general treatment of anisotropic photoelasticity to include the effects of an arbitrary residual birefringence is given by Knight and Pih [5]. Lately, the photoelasticity treatments of Hahn and Morris [7] and Hyer and Liu [8] also include the effects of the residual birefringence. Sullivan, Blais and Van Oene [9] verified Hyer and Liu's stress-optic law

‡ Author to whom all correspondence should be addressed.

on centrally loaded generally and specially orthotropic beams. Using this stress-optic law, their experimental results agreed with the theory excellently.

The key to dynamic analysis for orthotropic birefringent composites is obtaining a dynamic orthotropic stress-optic law. Although the dynamic stress-optic law and the static stress-optic law for isotropic materials are identical in form, the former is not extended simply from the latter. Large amounts of experimental researches were conducted by Frocht *et al.* [10, 11]; Clark *et al.* [12, 13] and Pih [14]. In the end, they proved that the dynamic stress-optic law is similar to the static law in form when the static stress-fringe value is replaced by the dynamic stress-fringe value. Reviewing researches on the dynamic stress-optic law for isotropic materials, we conclude that the stress-optic law is the same in form either in static case or in dynamic case. But, all parameters, which are related to time history, such as stresses and fringe orders in dynamic case, must be considered as variables of time. Also, the stress-fringe value must be calibrated in a homologous loading condition. That is, for the static stress-optic law, the stress-fringe value is calibrated in the static case and for the dynamic stress-optic law, the stress-fringe value is calibrated in the dynamic case.

Researches on dynamic stress-optic law for isotropic materials may be used for reference in obtaining the dynamic stress-optic law for orthotropic birefringent composites for the purpose of macroscopic analysis. Based on analogous consideration, the dynamic stress-optic law for orthotropic birefringent composites is postulated to be same in form to the one in the static case. As mentioned above, stresses and fringe orders are variables of time and the stress-fringe values must be calibrated in the dynamic case. Therefore, according to the static stress-optic law of Hyer and Liu [8], the dynamic stress-optic law for orthotropic birefringent composites in an xy coordinate system is

$$N_{\mathrm{T}} = \left\{ \left(\frac{\sigma_x}{C_1} - \frac{\sigma_y}{C_2} + \frac{\tau_{xy}}{C_3} + N_{\mathrm{R}} \cos 2\delta_{\mathrm{R}} \right)^2 + \left[2\left(\frac{\sigma_x - \sigma_y}{C_4} + \frac{\tau_{xy}}{C_5} \right) + N_{\mathrm{R}} \sin 2\delta_{\mathrm{R}} \right]^2 \right\}^{1/2} \quad (1)$$

where

$$\begin{aligned} 1/C_1 &= d\left(\frac{\cos^2\theta}{f_1} - \frac{\sin^2\theta}{f_2} \right) \\ 1/C_2 &= d\left(\frac{\cos^2\theta}{f_2} - \frac{\sin^2\theta}{f_1} \right) \\ 1/C_3 &= d(1/f_1 + 1/f_2)\sin 2\theta \\ 1/C_4 &= -\frac{d\sin\theta\cos\theta}{f_{12}} \\ 1/C_5 &= \frac{d(\cos^2\theta - \sin^2\theta)}{f_{12}} \end{aligned} \quad (2)$$

In Equations 1 and 2, N_{T} is the total observed birefringence, N_{R} is the residual birefringence, δ_{R} is the residual isoclinic angle in the material coordinate system, f_1, f_2 and f_{12} are dynamic stress-fringe values of the material, θ denotes the fiber angle referenced to the x axis and d is the thickness of the specimen. f_1 and f_2 denote photoelastic constants for the longitudinal and transverse directions, respectively, f_{12} is the shear photoelastic constant.

3. Experiments

3.1. Materials

Suitable model materials are necessary in the dynamic analysis for orthotropic birefringent composites. Firstly, this kind of material must have superior transparency, which directly affects the quality of birefringent fringe patterns. Dally *et al.* [1] previously found Cranz-Schardin cameras provide inadequate light to photograph transient events in the material they used then. They consequently employed pulsed-laser illumination and repeatability photography to record wave motion in this medium. Secondly, this kind of material should have higher homogeneity. Orthotropic photoelasticity is an experimental method which studies the mechanical behavior in orthotropic birefringent composites on a macroscopic scale. Homogeneity of material is not usually given close attention in the static analysis. However, complicated wave interactions would possibly arise in wave propagation because the composites are two phase materials in reality. Furthermore, in order to gain enough birefringent fringes, the material suitable for the dynamic analysis should possess higher photoelastic sensitivity than the material in the static analysis. It is well known that the photoelastic sensitivity of material under dynamic loading is usually much lower than that of material under static loading, and that the photoelastic sensitivity of the composite is usually lower than that of its resin matrix. Considering these factors, the birefringent composites with high fiber content are usually not utilized in the dynamic analysis and the higher standard is required in material fabrication.

Residual birefringence of composite must be taken into account in dynamic orthotropic photoelasticity as it influences stress distributions, birefringent fringe orders and the developing trend of birefringent fringes of the composite under dynamic loading. The residual birefringence is usually determined in a no-load condition. The residual isoclinic angle in the material coordinate system can be obtained in a plane polariscope and in a circular polariscope using white light successively. With Tardy method of compensation, the residual birefringent fringe orders can be obtained in a circular polariscope. The composites used in our investigation are made from unidirectional fiber-reinforced epoxy lamina with approximate 5% fiber content. The residual isoclinic angle, δ_{R}, was found to be 0 degree. This value is consistent with residual tension along the fiber in the matrix. The residual birefringent fringe order, N_{R}, was found to be less than one fringe order, specifically a value between 0.4 and 0.8. Although the residual birefringence is in the same level, it varies over the lamina. Thus, for a specific point in which we are interested, specific measurement must be conducted.

3.2. Calibrations

In static analysis, mechanical constants of orthotropic birefringent composites, E_1, E_2, G_{12}, ν_{12} and ν_{21}, are usually calibrated by three uniaxial tests. There are large differences between dynamic mechanical constants and static ones. To accurately determine the pulse loading in laboratory is not easy, so, for a rod under the loading of a one-dimension stress wave, finding a relation among the wave velocity, the elastic modulus and other parameters for orthotropic composites, similar to the relation among the wave velocity, the elastic modulus and the mass density for isotropic materials, is absolutely necessary. Fortunately, imitating the method for isotropic materials, this relation can be obtained as follow

$$c_{\mathrm{L}} = \sqrt{E_x/\rho} \tag{3}$$

where c_{L} denotes the dilatational wave velocity, E_x is the elastic modulus along the rod axis and ρ is the mass density of material.

It is apparent from an inspection of Equation 3 that this relation is identical in form with the expression for isotropic materials. However, the dilatational wave velocity is related only to the elastic modulus along the rod axis.

Three uniaxial specimens, 0°, 90° and 45° specimens, were fabricated to calibrate dynamic constants. A Cranz-Schardin camera was used to record dynamic fringe patterns. Meanwhile, longitudinal and transverse strains of specific point were obtained with dynamic strain measurements. We define the x axis to be along the rod axis and denote that θ is the angle between the xy coordinate system and the material coordinate system x_1y_1.

The dynamic poison's ratio is determined as follows

$$\nu_{21} = |\varepsilon_2(t)/\varepsilon_1(t)| \quad 0^\circ \text{ specimen} \tag{4}$$

$$\nu_{12} = |\varepsilon_1(t)/\varepsilon_2(t)| \quad 90^\circ \text{ specimen} \tag{5}$$

where $\varepsilon_1(t)$ and $\varepsilon_2(t)$ denote the strains at specific point for the longitudinal and transverse directions in the material coordinate system, respectively.

The dilatational wave velocity c_{L} can be determined from the relation

$$c_{\mathrm{L}} = s/\Delta t \tag{6}$$

where s is the distance between two specific points along the rod axis and Δt is the time interval of strain response for the two points.

When x direction is chosen as principal direction of material, Equation 3 becomes

$$E_1 = \rho c_{\mathrm{L1}}^2 \quad 0^\circ \text{ specimen} \tag{7}$$

$$E_2 = \rho c_{\mathrm{L2}}^2 \quad 90^\circ \text{ specimen} \tag{8}$$

when $\theta = 45^\circ$, Equation 3 becomes

$$E_{45^\circ} = \rho c_{\mathrm{L}45^\circ}^2 \quad 45^\circ \text{ specimen} \tag{9}$$

The shear modulus G_{12} can be obtained from the relation as follow

$$G_{12} = \frac{1}{\frac{4}{E_{45^\circ}} - \frac{1}{E_1} - \frac{1}{E_2} + \frac{2\nu_{21}}{E_1}} \tag{10}$$

According to above expressions, the constants E_1 and E_2 are determined from dynamic compressive tests on 0° and 90° specimens, respectively. The constants G_{12} is determined from the dynamic compressive test on 45° specimen in conjunction with other necessary parameters. The mass density ρ is considered to be constant in small strain condition.

When a rod is under compressive stress pulse, $\sigma_y = \tau_{xy} = 0$, $\sigma_x = E_x\varepsilon_x$, in conjunction with $\delta_{\mathrm{R}} = 0$, Equation 1 becomes

$$N_{\mathrm{T}} = |N_{\mathrm{R}} + dE_1\varepsilon_x/f_1| \quad 0^\circ \text{ specimen} \tag{11}$$

$$N_{\mathrm{T}} = |N_{\mathrm{R}} - dE_2\varepsilon_x/f_2| \quad 90^\circ \text{ specimen} \tag{12}$$

$$N_{\mathrm{T}} = \left[\left(N_{\mathrm{R}} + \frac{1}{2}dE_{45^\circ}\varepsilon_x\left(\frac{1}{f_1} - \frac{1}{f_2}\right)\right)^2 + \left(\frac{dE_{45^\circ}\varepsilon_x}{f_{12}}\right)^2\right]^{1/2} \quad 45^\circ \text{ specimen} \tag{13}$$

where ε_x is negative and denotes the compressive strain along the rod axis.

To solve stress-fringe values with Equations 11–13 is very complicated. Noticing that the history of fringe orders is linear and the strain history is also linear approximately before the first peak, when they are linearly curvefitted, Equations 11–13 much simplify to

$$f_1 = \frac{dE_1k_\varepsilon}{k_N} \quad 0^\circ \text{ specimen} \tag{14}$$

$$f_2 = \frac{dE_2k_\varepsilon}{k_N} \quad 90^\circ \text{ specimen} \tag{15}$$

$$f_{12} = \left[\left(\frac{k_N}{dE_{45^\circ}k_\varepsilon}\right)^2 - \frac{1}{4}\left(\frac{1}{f_1} - \frac{1}{f_2}\right)^2\right]^{-1/2} \quad 45^\circ \text{ specimen} \tag{16}$$

where $k_\varepsilon = \mathrm{d}\varepsilon_x(t)/\mathrm{d}t$, $k_N = \mathrm{d}N_{\mathrm{T}}(t)/\mathrm{d}t$ and they denote the slopes of the linearly curvefitted history of fringe orders and strain history, respectively.

It is obvious that the residual birefringence is not considered in calibration of all stress-fringe values. Knowing the histories of fringe orders, the strain histories and necessary parameters, f_1 and f_2 can be determined from dynamic compressive tests on 0° and 90° specimens, respectively. Subsequently, f_{12} can be

TABLE I Dynamic constants of the composites (with approximate 5% fiber content)

E_1 (GPa)	E_2 (GPa)	G_{12} (GPa)	ν_{21}	ν_{12}	f_1 (10^3 N/m · fringe)	f_2 (10^3 N/m · fringe)	f_{12} (10^3 N/m · fringe)
7.66	4.27	1.60	0.36	0.20	49.18	36.71	31.86

determined from dynamic compressive test on 45° specimen.

3.3. Uniaxial impact tests

A Cranz-Schardin camera is used broadly in dynamic photoelasticity. This camera is comprised of three basic subsystems which include: the spark-gap assembly, the optical bench and the control circuits for synchronization. The rifle was used to exert impact loading which has the loading rate of about 50 MN/sec. The composites studied herein were made from unidirectional fiber-reinforced epoxy lamina with approximate 5% fiber content. Dynamic constants of the composites were calibrated according to methods mentioned previously. These results are recorded in Table I.

The purpose of uniaxial impact tests is to verify the dynamic orthotropic stress-optic law proposed above in uniaxial-stress fields. Three calibration specimens, 0°, 90° and 45° specimens, 170 × 25 mm in size and 5 mm in thickness, were used. Two specific points, marked A and B, were chosen for each specimen. The distance from the top of the specimen to the specific point, A and B, is 85 mm and 120 mm, respectively. A foil strain gage was mounted on each specific point along the rod axis for each specimen. An ultra dynamic strain recorder, a transient waveform storage and an X-Y recorder were used in dynamic strain measurements. While dynamic birefringent fringe patterns were being recorded, strain histories for specific points were being obtained.

Several light-field birefringent fringe patterns are presented in Fig. 1.

3.4. Biaxial impact tests

The purpose of biaxial impact tests is to further verify the dynamic orthotropic stress-optic law in biaxial-stress fields. A plate of unidirectional fiber-reinforced birefringent composite under impact loading, with the loading direction parallel, perpendicular and at 45° to the fiber direction, was analyzed by dynamic photoelasticity, dynamic strain measurements and time domain BEM for anisotropic media. The plate, cut from the same material that was cut into three calibration specimens, was so large that there was no influence from reflection waves. For each of the loading directions, two three-gage 45-deg foil rosettes were mounted on the plate along the loading direction and two three-gage 45-deg foil rosettes were mounted on the plate along the line perpendicular to the loading direction, as shown in Fig. 2. The dynamic loading is similar to that in uniaxial impact tests. While dynamic birefringent fringe patterns were being recorded, strain histories for specific points, A, B, C and D, were being obtained for each loading direction. Several light-field birefringent fringe patterns for each loading direction are presented in Fig. 3.

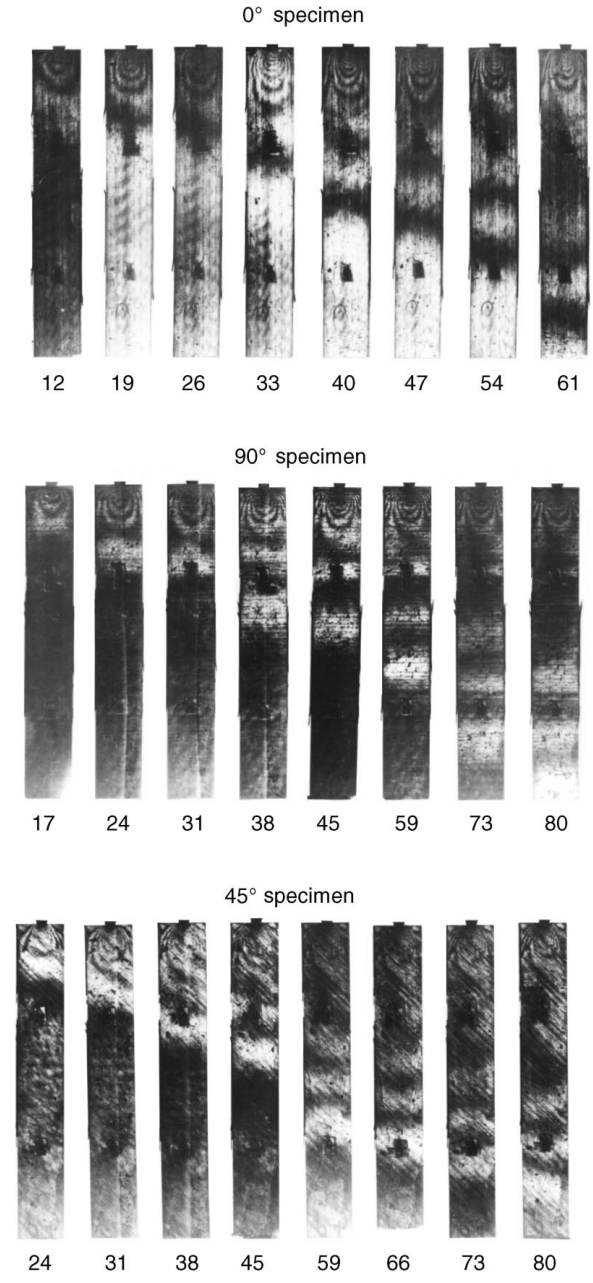

Figure 1 Several birefringent fringe patterns in the case of uniaxial stresses (Time unit: μs).

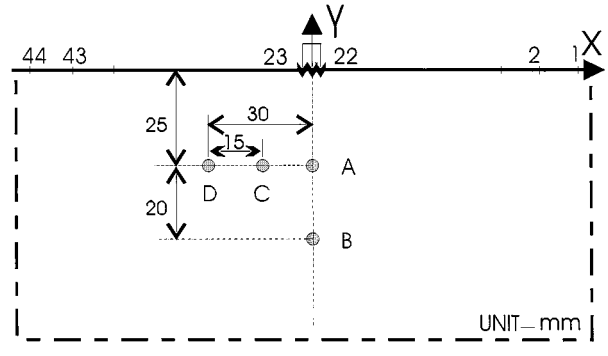

Figure 2 The composite plate under impact loading.

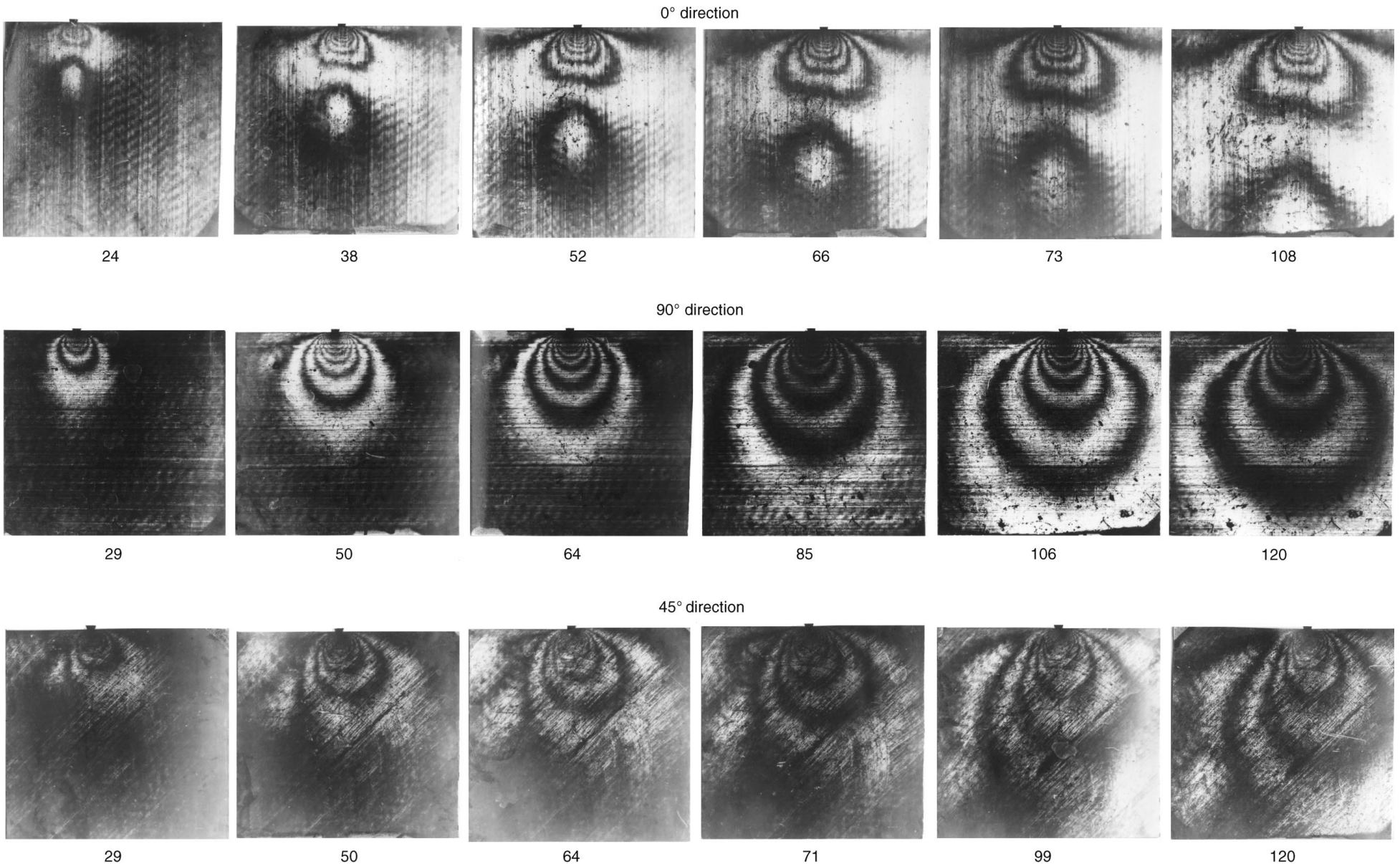

Figure 3 Several birefringent fringe patterns in the case of biaxial stresses (Time unit: μs).

4. Results and discussion

4.1. Uniaxial-stress fields

The stress component along the axis of the specimen, σ_x, calculated from dynamic stress-optic law, was compared with the result from dynamic strain measurements in uniaxial compressive condition. When a rod is under compressive stress pulse, $\sigma_y = \tau_{xy} = 0$, $\sigma_x = E_x \varepsilon_x$, in conjunction with $\delta_R = 0$, Equation 1 becomes

$$\sigma_x = \frac{(\pm N_T - N_R) f_1}{d} \quad 0^\circ \text{ specimen} \tag{17}$$

$$\sigma_x = \frac{(N_R \pm N_T) f_2}{d} \quad 90^\circ \text{ specimen} \tag{18}$$

In Equations 17 and 18, $N_T \geq 0$, $N_R \geq 0$ and σ_x denotes the stress component along the axis due to the applied load if $-N_T$ is chosen.

For the 45° specimen, the equation about σ_x is

$$a\sigma_x^2 + b\sigma_x + c = 0 \tag{19}$$

where

$$a = d^2 \left[\frac{1}{f_{12}^2} + \frac{1}{4}\left(\frac{1}{f_1} - \frac{1}{f_2} \right)^2 \right]$$

$$b = d N_R \left(\frac{1}{f_1} - \frac{1}{f_2} \right) \tag{20}$$

$$c = N_R^2 - N_T^2$$

Thus, σ_x is obtained as follow

$$\sigma_x = \frac{-b \pm \sqrt{b^2 - 4ac}}{2a} \tag{21}$$

In Equation 21, σ_x denotes the stress component along the axis due to the applied load if σ_x is negative.

The residual birefringence influences stress distributions, birefringent fringe orders and the developing trend of birefringent fringes of composites under dynamic loading. Using the dynamic stress-optic law, the approximate residual stress along the fiber, in the case of uniaxial stresses, can be obtained

$$\sigma_R = \frac{N_R f_1}{d} \tag{22}$$

The tensile residual stress must be considered in calculations of the stress due to the applied load in dynamic strain measurements. For the 0° specimen, the stress due to the applied load countervails the residual stress because the former deviates from the latter. For the 90° specimen, the stress due to the applied load folds the residual stress because the former is along the latter. For the 45° specimen, tensile residual stress along the axis, $\sigma_R/2$, is induced by the tensile residual stress along the fiber and it countervails the stress due to the applied load. The influences of residual birefringence on total birefringence also must be considered in the analysis of birefringent fringe patterns. If the residual

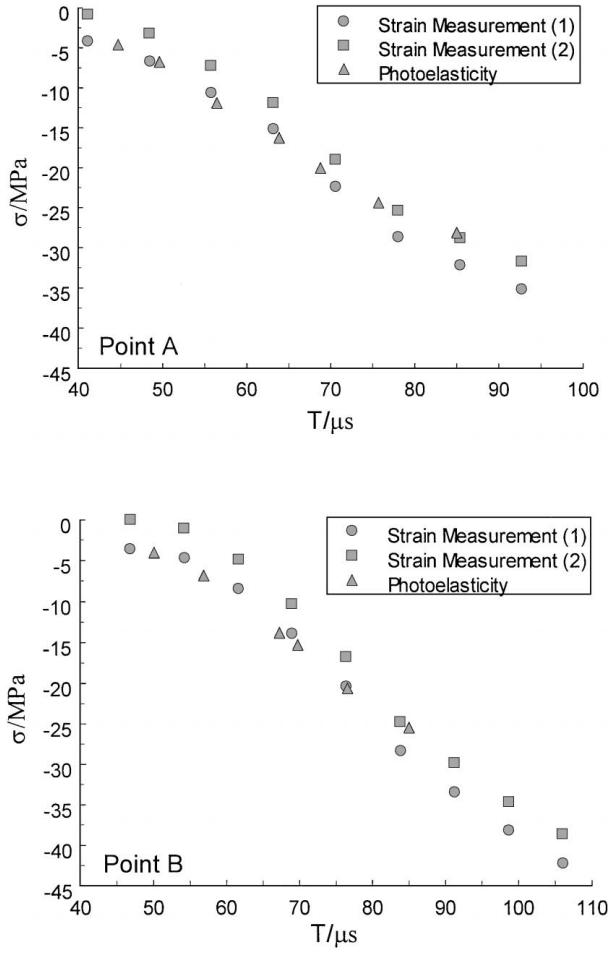

Figure 4 The stress histories for specific points (0° specimen) .

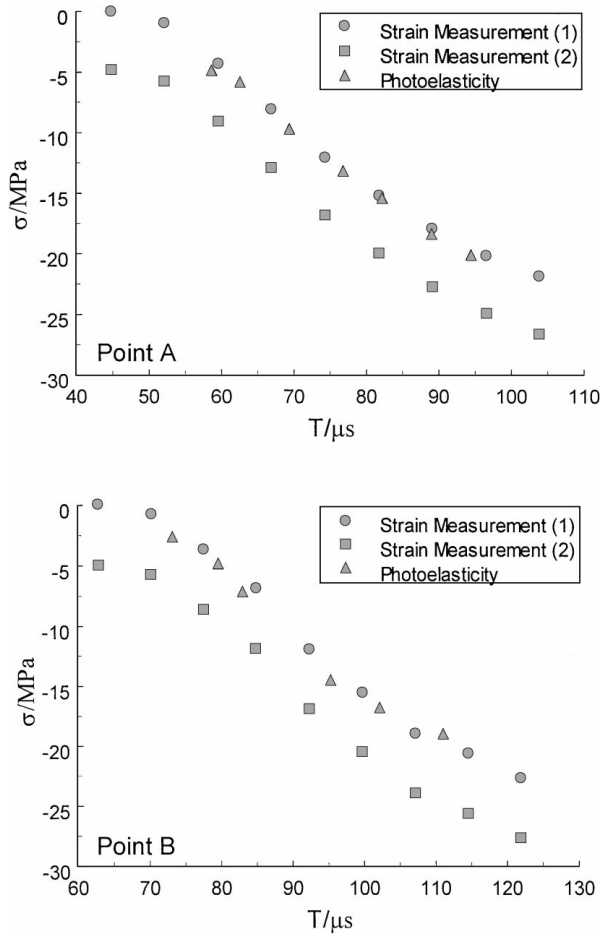

Figure 5 The stress histories for specific points (90° specimen).

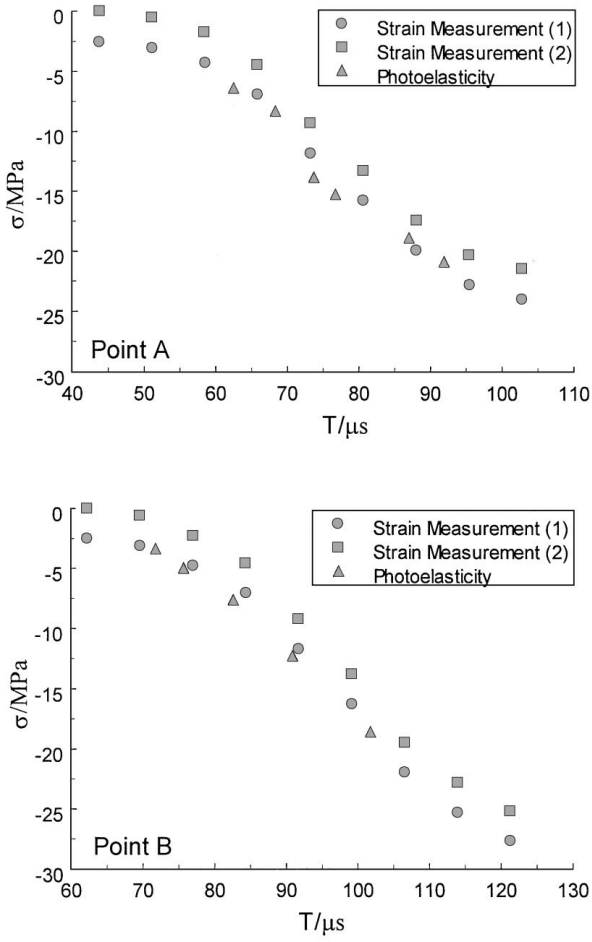

Figure 6 The stress histories for specific points (45° specimen).

birefringence, due to a residual tension in the fiber direction, is assumed to be less than the first order, the sequence of fringes observed for the 0° specimen is (0, 1, 2, 3) and the sequences of fringes observed for the 90° specimen and 45° specimen are all (1, 2, 3, 4). If the residual birefringence is assumed to be between the first and second orders, then the sequence for the 0° specimen is (1, 0, 1, 2) and the sequences for the 90° specimen and 45° specimen are all (2, 3, 4, 5).

The stresses at specific points, for each loading direction, were calculated from dynamic orthotropic photoelasticity and dynamic strain measurements, respectively. Two methods, the first including the residual stress and the second not including the residual stress, were accepted in analysis of dynamic strain measurements. The results are presented in Figs 4–6. Inspecting from these figures, it is obvious that the results, including the residual stress in dynamic strain measurements, are very close to the results from dynamic orthotropic photoelasticity.

4.2. Biaxial-stress fields

The composite plate under impact loading, with the loading direction parallel, perpendicular and at 45° to the fiber direction, was analyzed by dynamic orthotropic photoelasticity, dynamic strain measurements and time domain BEM for anisotropic media. The history of birefringent fringe orders for each specific point in each loading direction, calculated from the dynamic stress-optic law making use of stress values from strain

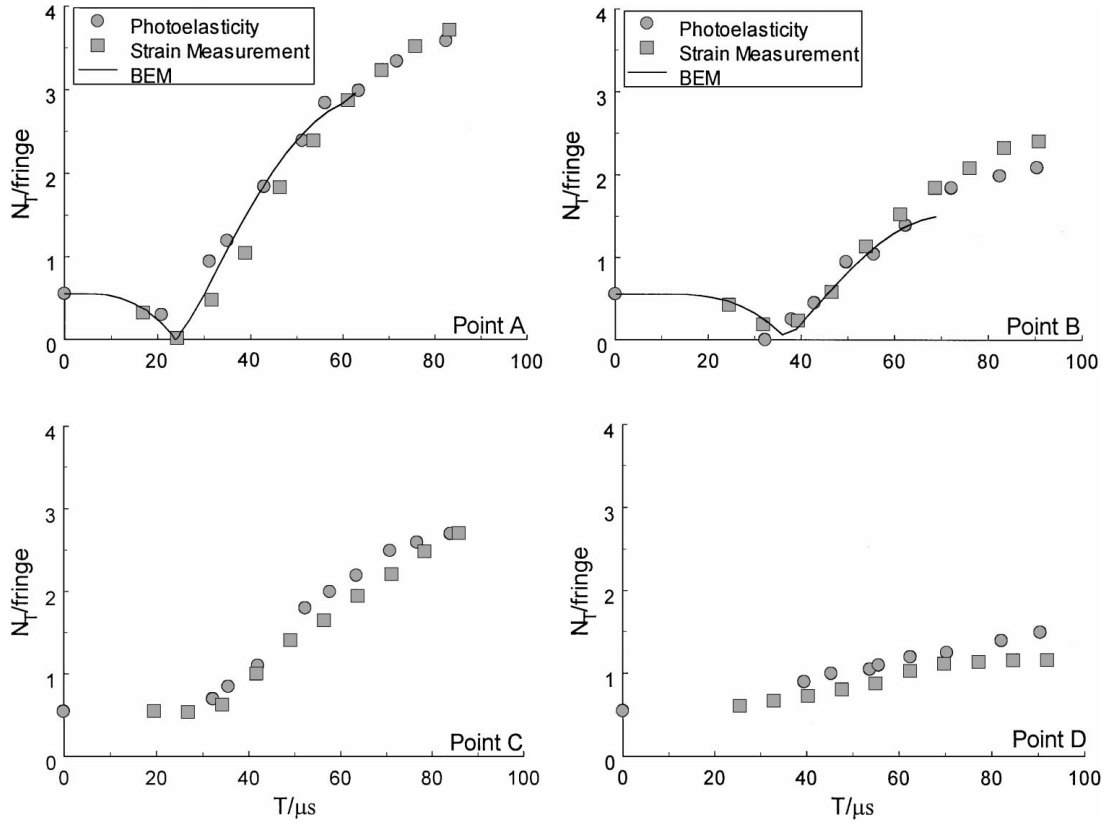

Figure 7 The histories of birefringent fringe orders for specific points (0° direction).

measurements and BEM calculations respectively, was presented and compared with the result of dynamic orthotropic photoelasticity.

In analysis of dynamic strain measurements, the stress components at specific point were converted from the strain components at the point according to stress-strain relations under plane stress conditions. Substituting calculated stresses into Equation 1, the histories of birefringent fringe orders for specific points can be obtained, as shown in Figs 7–9.

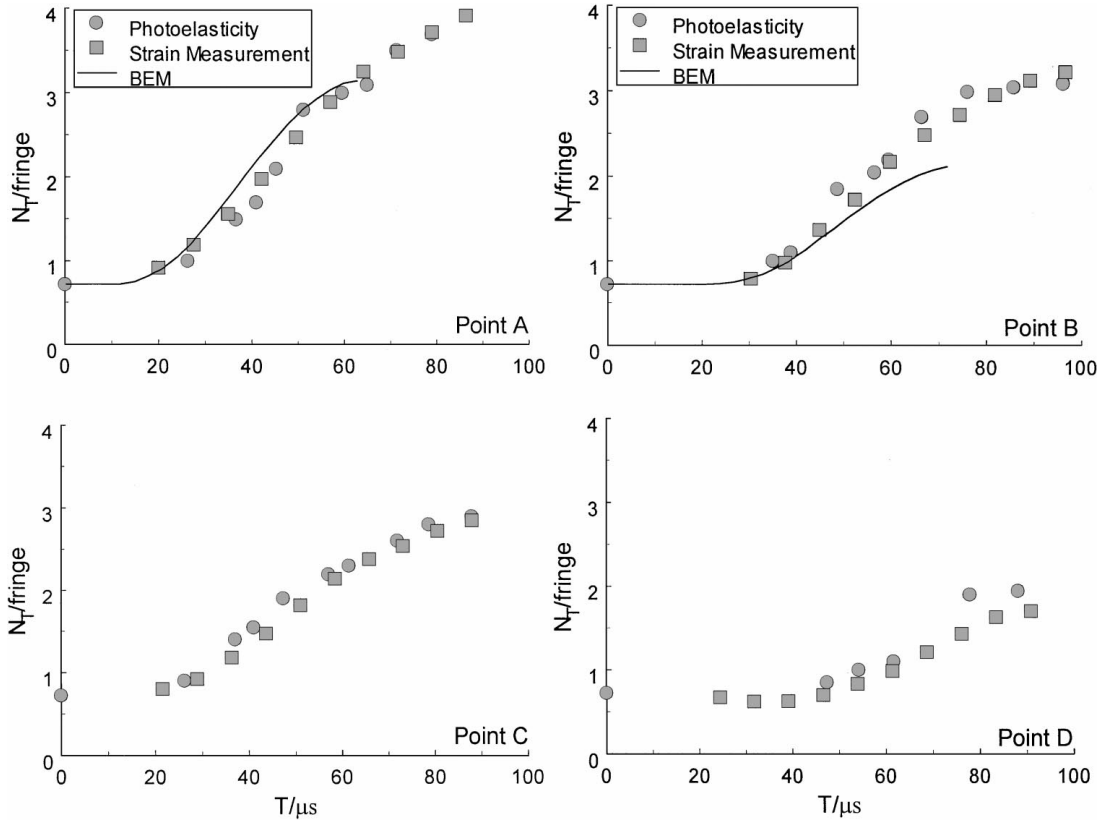

Figure 8 The histories of birefringent fringe orders for specific points (90° direction).

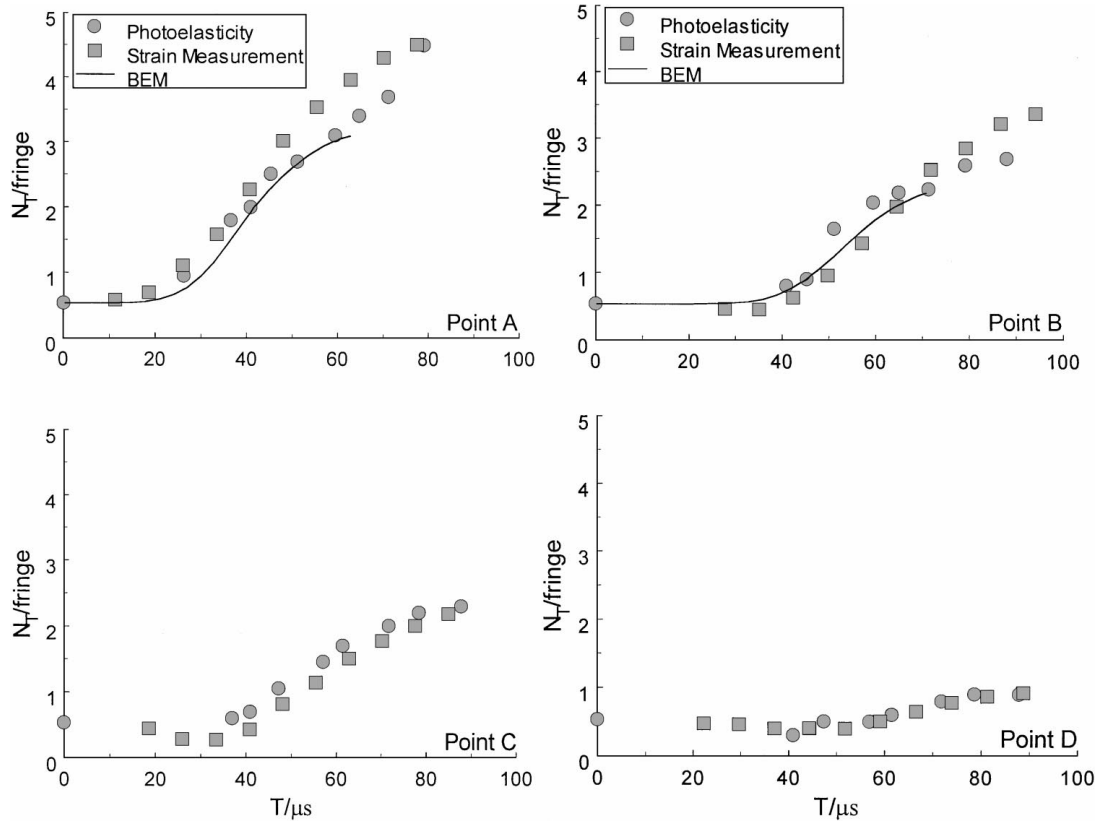

Figure 9 The histories of birefringent fringe orders for specific points (45° direction).

The time domain Boundary Element Method for wave propagation problems in anisotropic media was used solving stresses at specific points along the loading direction. The Boundary Element Method (BEM) has become increasingly popular for the solution of linear elastodynamic problems. Its popularity can be attributed primarily to the reduction of dimensionality of problems, high accuracy of results and automatic consideration of the radiation conditions at infinity. Because it obtains transient response of the system directly, time domain BEM for anisotropic media is the better numerical method for solving dynamic response of the system under detonation or impact loading.

In analysis with time domain BEM, the composite plate was considered to be half-plane under applied surface load, with the loading direction parallel, perpendicular and at 45° to the fiber direction. The interface, which is 0.4 m in length, was discretized into 43 linear elements, as shown in Fig. 2. The largest element size, l_j, is 0.01 m and the time increment, Δt, is 3 μs. The parameter, $C_{\mathrm{I}}\Delta t/l_j$, is between 0.4 and 0.8, where C_{I} denotes the dilatational wave velocity. The loading curve necessary for calculations was calibrated on site. Substituting calculated stresses into Equation 1, the histories of birefringent fringe orders for specific points can be obtained, as shown in Figs 7–9.

5. Conclusions

Dynamic photoelastic analysis for orthotropic birefringent composites, namely dynamic orthotropic photoelasticity, is investigated in this paper. The birefringent composites suitable for the dynamic analysis, the effects of residual birefringence, dynamic orthotropic stress-optic law and calibrations of dynamic mechanical constants and dynamic stress-fringe values, are four fundamental problems in this study. For model materials, superior transparency, higher homogeneity and photoelastic sensitivity than in the static analysis are necessary in the dynamic analysis. Residual birefringence influences stress distributions, birefringent fringe orders and the developing trend of birefringent fringes of composites under dynamic loading. Therefore, it must be considered either in the form of the dynamic stress-optic law or in determining the sequence of fringes observed for the specimen. The stress-optic law for dynamic photoelastic analysis of orthotropic birefringent composites is postulated based on the static stress-optic law of Hyer and Liu. Then, practical methods of calibrating dynamic mechanical constants and dynamic stress-fringe values are proposed. Using three calibration specimens, uniaxial impact tests were conducted to verify the proposed law in uniaxial-stress fields. The stresses at specific points including the residual stress, calculated from dynamic strain measurements, are very close to the results from dynamic orthotropic photoelasticity. It demonstrates not only the large effects of the residual birefringence but also the validation of the employed dynamic stress-optic law in uniaxial-stress fields. Biaxial impact tests were conducted to further verify the dynamic stress-optic law. A composite plate under impact loading, with the loading direction parallel, perpendicular and at 45° to the fiber direction, was analyzed with dynamic orthotropic photoelasticity, dynamic strain measurements and time domain BEM for anisotropic media. The history of birefringent fringe orders for each specific point in each loading direction, calculated from the dynamic stress-optic law making use of stress values from strain measurements and BEM calculations respectively, was compared with the result of dynamic orthotropic photoelasticity. Considering that some factors may influence the experimental results and BEM calculations, such as the determination of the impact loading, calibrations of dynamic mechanical constants and dynamic stress-fringe values and data reading from the fringe patterns and strain curves, the agreement among these three results is good. This serves as further validation of the proposed dynamic orthotropic stress-optic law in biaxial-stress fields.

Acknowledgement

Financial support of this work was supported by the National Science Foundation of China under Grant No. 19572035 and National Key Projects on Basic Research: Applied Research on Safety and Durability of Major Construction Projects. Appreciation is also expressed to Prof Su X.J., Department of Mechanics, Beijing University, Prof Song J.L., Department of Mechanical Engineering, Tianjin University and Prof Dai F.L., Department of Engineering Mechanics, Tsinghua University for their valuable suggestions to this study.

References

1. J. W. DALLY, J. A. LINK and R. PRABHAKARAN, in Proceedings of the 12th Midwestern Mechanics Conference, 1971, pp. 937–949.
2. R. E. ROWLANDS, I. M. DANIEL and R. PRABHAKARAN, *Experimental Mechanics* **14**(11) (1974) 433–439.
3. J. CERNOSEK, *Experimental Mechanics* **15**(9) (1975) 354–357.
4. R. K. MITTAL, *Strain* **11** (1975) 55–57.
5. C. E. KNIGHT and H. PIH, *Fibre Sci. Technol.* **9** (1976) 297–313.
6. S. K. CHATURVEDI, *Int. J. Eng. Sci.* **20**(1) (1982) 145–157.
7. H. T. HAHN and D. H. MORRIS, *Fibre Sci. Technol.* **11** (1978) 113–125.
8. M. W. HYER and D. H. LIU, NASA Rep. 3773, 1984.
9. J. L. SULLIVAN, E. BLAIS and H. VAN OENE, *Experimental Mechanics* **27**(6) (1987) 208–219.
10. M. M. FROCHT, A. A. BETSER and P. D. FLYNN, *Proc. of the Ninth Intl. Congress for Theory and Appl. Mech.* **8** (1957) 367–377.
11. M. M. FROCHT, in "Proc. of Intl. Symposium on Stress Wave Propagation in Materials," edited by Norman Davis (Inter Science, New York, 1960) pp. 91–118.
12. A. B. J. CLARK, *SESA Proc.* **14**(1) (1956) 195–204.
13. A. B. J. CLARK and R. J. SANFORD, *Experimental Mechanics* **4**(6) (1963) 148–151.
14. H. PIH, *Experimental Mechanics* **4**(2) (1963) 33–40.

Received 28 January
and accepted 20 August 1998